



## Corrosion Inhibition Efficiency of Pistachio Galls Extract of X70 Steel in H<sub>2</sub>SO<sub>4</sub> 1 N

M Ferhat<sup>1\*</sup>, M Kacheba<sup>1</sup>, AS Benmebarek<sup>1</sup> and M Yousfi<sup>2</sup>

<sup>1</sup>Mechanic Laboratory, University of Laghouat-Ghardaia Road, Laghouat, Algeria

<sup>2</sup>Laboratory of Fundamental Sciences, University Amar TĒLIDJI of Laghouat, Ghardaïa Road, Laghouat, Algeria

### ABSTRACT

The aim of this work is to use a natural substance recovered from pistachio galls as anticorrosion agent, another opportunity to exploit natural resources. The present study investigates the inhibiting effect of extracts from pistachio galls of Atlas. Electrochemical methods associated with the infrared Fourier transform spectroscopy are used. The results show that this substance can be used as an ingredient for the design of a new family of greener and less costly inhibitors. The Electrochemical study showed that pistachio galls act in electrostatics interaction with the steel surface, and thus by physical adsorption. The analysis FTIR spectroscopy confirms this result.

**Keywords:** Corrosion; Green inhibitor; Steel X70; EIS; FTIR

### INTRODUCTION

Corrosion is both costly and dangerous. Billions of dollars are spent annually for the replacement of corroded structures, machinery, and components, including metal roofing, condenser tubes, pipelines, and many other items. In addition to replacement, costs are those associated with preventive maintenance to prevent corrosion. In the oil extraction and processing industries, Inhibitors have always been considered to be the first defense line against corrosion. A great number of scientific studies have been devoted to the subject of corrosion inhibitors.

By definition, corrosion inhibitor is a chemical substance that, when added in small concentration to an environment, effectively decreases the corrosion rate. Additions of certain chemicals are made to the environment; nevertheless, most of these synthetic organic compounds are not only expensive but also toxic for live beings. Now, the restrictive environmental regulations have made researchers to focus on the need to develop cheap, non-toxic and environmentally benign natural corrosion inhibitors, with the increasing awareness of environmental pollution problems. This often places severe restrictions on the choice of inhibitor. The disposal of chromate and phosphate inhibitor formulations is important in this respect and there is an increasing move towards the low-chromate-phosphate types of formulation. In fact for some applications even this approach is not acceptable and inhibitor formulations containing bio-degradable chemicals are being introduced. These toxic effects have led to the use of natural products as anticorrosion agents which are eco-friendly and harmless. Some researcher groups have reported the successful use of naturally occurring substances (e.g. plant extracts) as green corrosion inhibitors for metallic materials in various corrosives media. Gece [1] has pointed out the same conclusion in using the drugs. Lately alternative eco-friendly corrosion inhibitors are developed, they range from rare earth elements [1-3] to organic compound [4,5]. Since 1930, plant extracts (dried stems, leaves and seeds) of Celandine (*Chelidonium majus*) and other plants were used in H<sub>2</sub>SO<sub>4</sub> pickling baths [6]. A Djemoui et al. [7] reported that alkaloids *extract from Peganum harkmala* give adequate protection to 6063 aluminium alloy in 1 M HCl in a temperature range 25 to 40°C LK Ojha et al. [8] found that Fenugreek leaves extract could be good inhibitors for mild-steel in a 1M

sulphuric acid. In fact, the first patented corrosion inhibitors used were either natural product such as flour, yeast etc. [9], or by products of food industries for restraining iron corrosion in acid media [10].

The originality of this study is the valorization of an organic substance, since it comes from a disease that reaches the pistachio "(Pistacia atlantica Desf.)". Pistachios are very prone to developing some defensive excrescences called gall or cecidia, to protect plant against attacks by parasites. These lay eggs in these formation and larvae feed on them instead on the plant tissues. Galls can take different shapes and sizes depending on different species but they are consisting of outgrowths developed in the leaves of these plants where these parasites lodge. The leaves and branches often have galls on the tree infested with gall-producing species. Some authors have devoted their study to the phytochemical and microbiological valorization of Atlas Pistachio galls [11,12]. Their work shows that pistachio galls are very rich in organic molecules, which are widely studied and used as corrosion inhibitors, often-containing nitrogen, oxygen and sulfur atoms, as well as multiple bonds in their heteroatom molecules, hence the interest in testing this substance. The use of pistachio galls to inhibit corrosion of carbon steel has not been reported in the literature. The objective is to extract the essential oil from these galls and to study their anticorrosive properties on X70 steel. In addition, this study highlights the effect of the extraction method and the solvent used.

## MATERIALS AND METHODS

### Preparation of Plant Extract

The natural substance provide from the pistachio galls of the Atlas from the El-Ghicha-Laghouat region (400 km south of Algiers). To obtain an essential oil, this was subsequently used to study the corrosion inhibition properties of X-70 steel in Sulfuric acid solution. Different solvents are used: Dichloromethane, Petroleum Ether, Methanol, Dimethylsulfoxide, Anhydrous sodium and Ethyl acetate. The extraction was carried out according two methods: Maceration and Soxhlet.

### Maceration method:

The galls of the Atlas pistachio are cleaned, dried for three days in an oven (40°C), and ground into fine powder. 10 g of the natural substance was macerated twice with extraction solvent (solvent/distilled water; v/v: 7/3) in an Erlenmeyer flask (2000 mL) with stirring, and renewing of the solvent every 24 hours at room temperature. After filtering the mixture, solvent is removed by rotary evaporator. Then liquid-liquid extraction is used with three solvent: petroleum ether, ethyl acetate and acetone.

### Soxhlet method:

60.37 g of Atlas pistachio gall powder are placed in a cellulose cartridge in the Soxhlet extractor body, attached to the flask containing the solvent, reflux heated for 5 to 6 hours. Four solvents are used in this method; petroleum ether, dichloromethane, acetone and methanol. After completion of the extraction, the solvent is removed using a rotary evaporator at 50°C. The obtained extracts are dried at open air.

All the obtained extracts are stored at 4°C. The essential oil content is defined as the ratio between the mass of essential oil obtained and the dry mass of the treated plant (eq.1). Table 1 summarizes the different content obtained:

$$R\% = \frac{\text{mass of the extract}}{\text{mass of plant matter}} \times 100 \quad (1)$$

Table 1 shows that Soxhlet extraction generally provides better yields than maceration method. In addition, using methanol solvent with Soxhlet method provides the highest percentage. All the obtained extracts are analysed by FTIR (Figure 1). The FTIR spectra show practically the same appearance for all the solvents used; these spectra therefore correspond to natural substance only. The solvent used does not interfere with inhibition process; this implies that only natural substance molecules will interact with the surface of the metal.

Only four extracts are retained for the electrochemical study: MS2, SS1, SS2 and SS4. The obtained quantities for the other extracts were insufficient to give significant inhibition efficiency.

### Electrochemical/Corrosion Cell and Equipment

The X-70 steel, has undergone several stages of preparations; cutting from the HAZ (Heat Affected Zone) of the welding zone of the pipeline. The sample was cut according to a square geometry and the exposed area was (1x1) cm<sup>2</sup>. The alloy are mechanically polished with emery paper up to 1200 grit, degreased in acetone, rinsed with bidistilled water, dried and transferred quickly in a Tacussel glass cell filled with 100 mL of 1N sulfuric acid solution. A saturated calomel reference electrode (SCE) and graphite electrode are used as reference and auxiliary electrodes respectively. All potentials in this paper refer to the SCE. At each potentiodynamic polarization, the samples are kept at the free corrosion potential for 30 mn and then the polarization responses are measured from ±

250 with respect to the corrosion potential in 1 N sulfuric acid medium conducted at a sweep rate of 0.5 mV/s [13]. The corrosion behaviour of the samples was evaluated by using an SP 150 Bio-logic Potentiostat/Galvanostat, monitored EC-Lab V10.44 software electrochemical. Impedance spectroscopy (EIS) was measured, and recorded at open circuit potentials, in the frequency ranging from 100 kHz to 10 mHz, with a sinusoidal signal perturbation of 10 mV. All electrochemical technics were thermostatically conducted at 25°C.

**Table 1: Yield of extraction solvent**

Method	Extraction Solvent		Abbreviation*	Weight of the extract (g)	Yield R%
Maceration	Petroleum ether	EX.M(P.E)	MS1	0.02	0.28
	Ethyl acetate	EX.M(A.E)	MS2	0.28	2.74
	Acetone	EX.M(Acetone)	MS3	0.33	3.3
Soxhlet	Petroleum Ether	EX.S(P.E)	SS1	2.5	4.14
	Dichloromethane	EX.S(DCM)	SS2	0.7	4.35
	Acetone	EX.S(Acetone)	SS3	0.53	0.87
	Methanol	EX.S(Methanol)	SS4	11.38	18.87

\*MS: Maceration Solvent; SS: Soxhlet Solvent

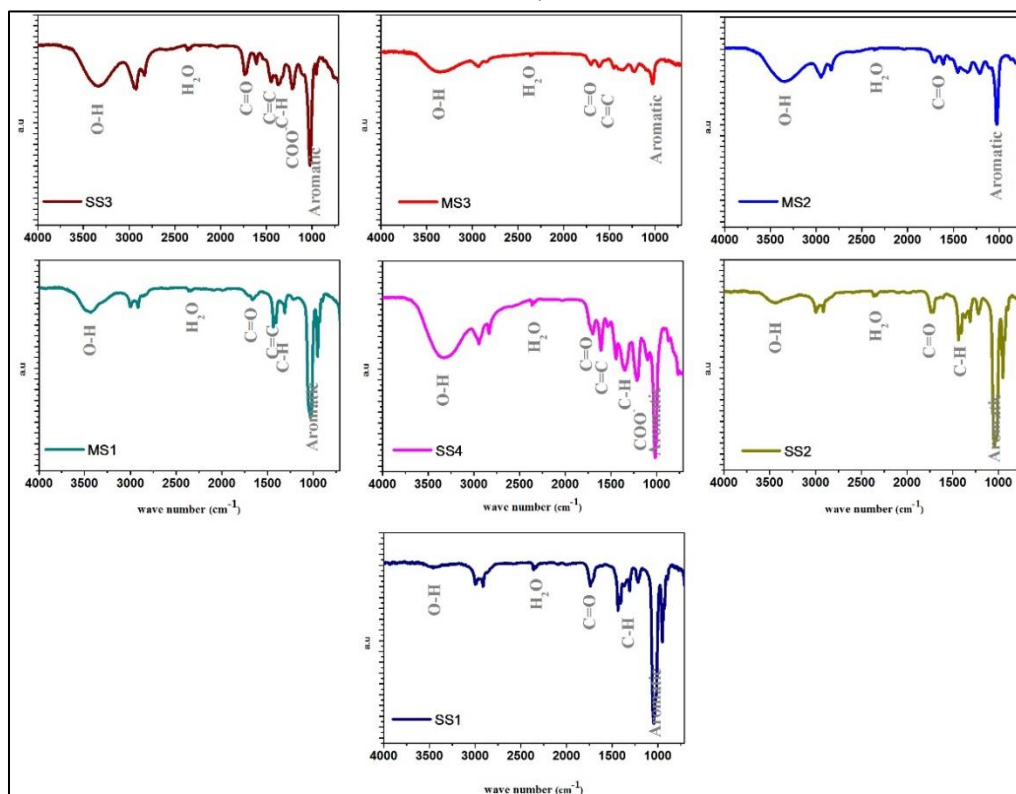


**Figure 1: FTIR spectra of the essential oil extracted with different solvents**

Fourier Transform Infrared spectra (FTIR) were recorded in a Perkin–Elmer–1600 spectrophotometer equipped with LITA detector. The product to be analyzed is mixed with oven-dried spectroscopic grade KBr and pressed into a vacuum pellet. The transmittance spectrum of the samples is recorded in triplicate by accumulating 512 sweeps at a resolution of 4 cm<sup>-1</sup> between 400 cm<sup>-1</sup> and 4000 cm<sup>-1</sup>.

## RESULTS AND DISCUSSION

## Electrochemical Impedance Spectroscopy

Electrochemical impedance spectroscopic (EIS) studies have been conducted to investigate corrosion inhibition processes in terms of the resistive as well as capacitive behavior at metal/solution interface. Figure 2 shows the Nyquist plots X70 steel in 0.5 M H<sub>2</sub>SO<sub>4</sub> solution with and without different concentrations of the natural extract for each solvent. The Nyquist plots were regarded as one part of a semicircle.

All the impedance diagrams were analyzed in terms of the equivalent circuit represented in Figure 3, which is a parallel combination of  $R_{ct}$  and the constant phase element of double layer (CPE), both in series with the solution resistance ( $R_e$ ). The charge transfer resistance values ( $R_{ct}$ ) were calculated from the difference in impedance at lower and higher frequencies, as suggested by Hamdi et al. [14].

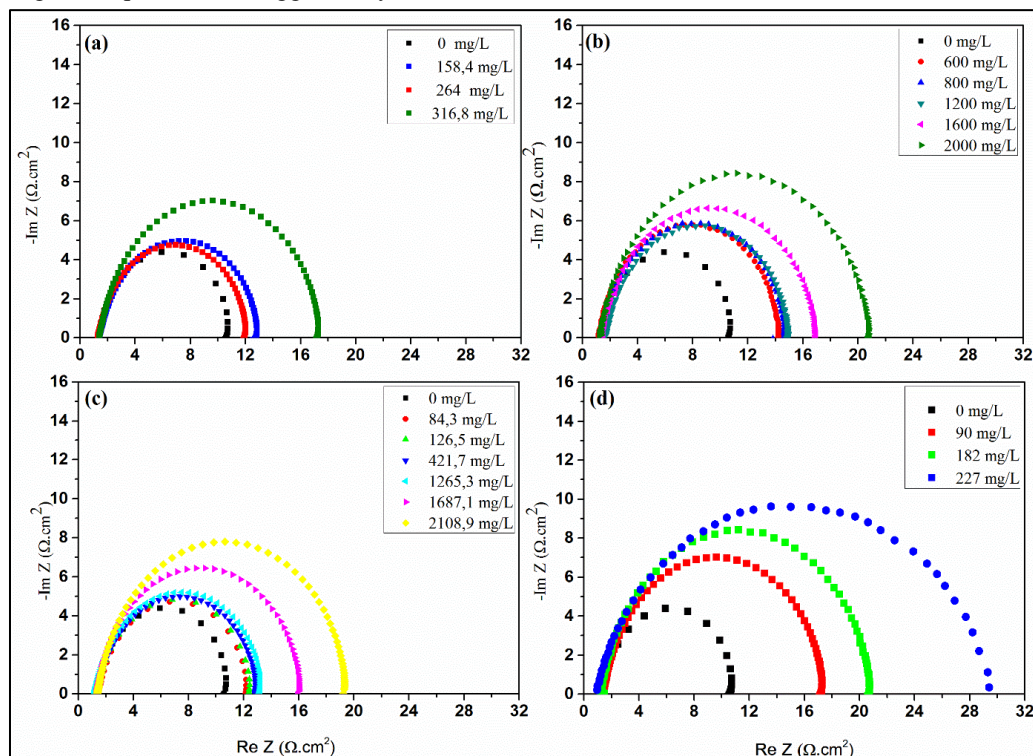


Figure 2: Nyquist diagram of X70 / H<sub>2</sub>SO<sub>4</sub> system at different concentration of extract: MS2 (a), SS1 (b), SS2 (c) and SS4 (d)

Generally, a large charge transfer resistance is associated with a slower corroding system. In contrast, better protection provided by an inhibitor can be associated with a decrease in capacitance of the metal/solution interface. To obtain the double layer capacitance  $C_{dl}$ , values were calculated from the following equation [15]:

$$C_{dl} = \frac{1}{2\pi f_{max} R_{ct}} \quad (2)$$

$f_{max}$  is the frequency at maximum imaginary component of the impedance. In case of the electrochemical impedance spectroscopy, inhibition efficiencies  $\eta$  were calculated using charge transfer resistance according to the following equation [16]:

$$\eta\% = \frac{R_{ct} - R_{ct}^0}{R_{ct}} * 100 \quad (3)$$

Where  $R_{ct}$  and  $R_{ct}^0$  are the charge transfer resistance values with and without inhibitor for X70 in 0.5 M H<sub>2</sub>SO<sub>4</sub>, respectively. The surface fraction occupied by adsorbed molecules ( $\theta$ ), i.e. the surface coverage of natural substance, is obtained by the ratio ( $\eta/100$ ).

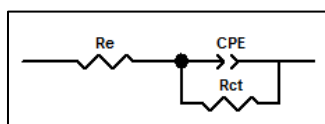


Figure 3: Equivalent circuit used to simulate the EIS diagrams presented in Figure 2

The impedance diagrams recorded in Nyquist mode at the open circuit potential show a single time constant for all concentrations. The analysis of the diagrams shows that the increase in the concentration induces an increase in the size of the capacitive loop. The capacitance,  $C_{dl}$ , values were decreased due to a decrease in local dielectric constant and/or an increase in the thickness of the electrical double layer, suggesting that the inhibitor molecules acted by adsorption at the metal/solution interface. The lower  $C_{dl}$  values are probably a consequence of replacement of water molecules by inhibitor molecule at the electrode surface. In addition, the inhibitor molecules may reduce the capacitance by increasing the double layer thickness according to the Helmholtz model [17]:

$$e = \frac{\epsilon\epsilon_0}{C_{dl}}A \quad (4)$$

Where  $\epsilon$  the dielectric constant of the medium is,  $\epsilon_0$  is the vacuum permittivity,  $A$  is the electrode surface area and  $e$  is the thickness of the protective layer.  $C_{dl}$  value was always smaller in the presence of the inhibitor than in its absence, which may be resulted from the effective adsorption of the natural inhibitors. It is observed that  $R_e$  (electrolyte resistance) is very small in each case, which again confirms that the IR drop could be small. From Table 2, it is clear that the addition of extract decreases the double layer capacitance and increases the charge transfer resistance; as consequence, a large diameter of the semicircle is observed in Nyquist plots. The decrease in  $C_{dl}$  could be attributed to the adsorption of the inhibitors on the electrode surface, forming protective adsorption layers. These findings indicate that, extract inhibit X70 steel corrosion by adsorption. As, the impedance spectra show one capacitive loop, adsorption of extract occurs by simple surface coverage and extract acts as a primary interface inhibitor [18].

The inhibiting efficiency was in the following order: SS4 > SS1 > SS2 > MS2. The gall extract prepared by the Soxhlet method using methanol solvent gives the best inhibition efficiency.

**Table 2: Values of the elements of equivalent circuit required for fitting the EIS for X70 / H<sub>2</sub>SO<sub>4</sub> system at different concentration of extract**

Extract	C (mg/L)	R <sub>e</sub> (Ω.cm <sub>2</sub> )	R <sub>ct</sub> (Ω.cm <sub>2</sub> )	C <sub>dl</sub> (μF.cm <sup>-2</sup> )	n	η %	Θ
Blank	0	1.31	9.63	699	0.92	-	-
MS2	158.4	1.29	10.99	369	0.89	12.37	0.12
	264	1.39	11.78	325	0.87	18.25	0.18
	316.8	1.21	15.99	305	0.9	39.77	0.4
SS1	600	1.23	13.22	304	0.91	27.16	0.27
	800	1.37	13.45	293	0.9	28.4	0.28
	1200	1.71	13.41	314	0.89	28.19	0.28
	1600	1.41	15.73	311	0.88	38.78	0.39
	2000	1.26	19.75	289	0.89	51.24	0.51
SS2	84.3	1.48	10.99	374	0.88	12.37	0.12
	126.5	1.34	11.31	348	0.88	14.85	0.15
	421.7	1.35	11.8	356	0.88	18.39	0.18
	1265.3	1.21	12.31	349	0.88	21.77	0.22
	1687.1	1.23	15.11	329	0.88	36.27	0.36
	2108.9	1.39	18.24	272	0.89	47.2	0.47
SS4	90	1.32	17.28	144	0.91	44.27	0.44
	182	1.29	19.33	121	0.92	50.18	0.5
	227	1.31	30.92	113	0.89	68.86	0.69

### Potentiodynamic Polarization Measurements

Figure 4 represents the potentiodynamic polarization curves of carbon steel (X70) in 0.5 M H<sub>2</sub>SO<sub>4</sub> in the presence and absence of various concentrations of natural substance extracted with different solvents. The electrochemical parameters, corrosion current density ( $i_{cor}$ ), corrosion potential ( $E_{cor}$ ), anodic Tafel slope ( $\beta_a$ ) and cathodic Tafel

slope ( $\beta_c$ ) and the inhibition efficiency ( $E\%$ ), at different inhibitor concentrations are listed in Table 3. The inhibition efficiency ( $E\%$ ) were calculated from the equation [19]:

$$E\% = \frac{i_{cor}^0 - i_{cor}}{i_{cor}^0} * 100 \quad (5)$$

Where,  $i_{cor}^0$  and  $i_{cor}$  are the corrosion current densities in the absence and presence of the inhibitor respectively.

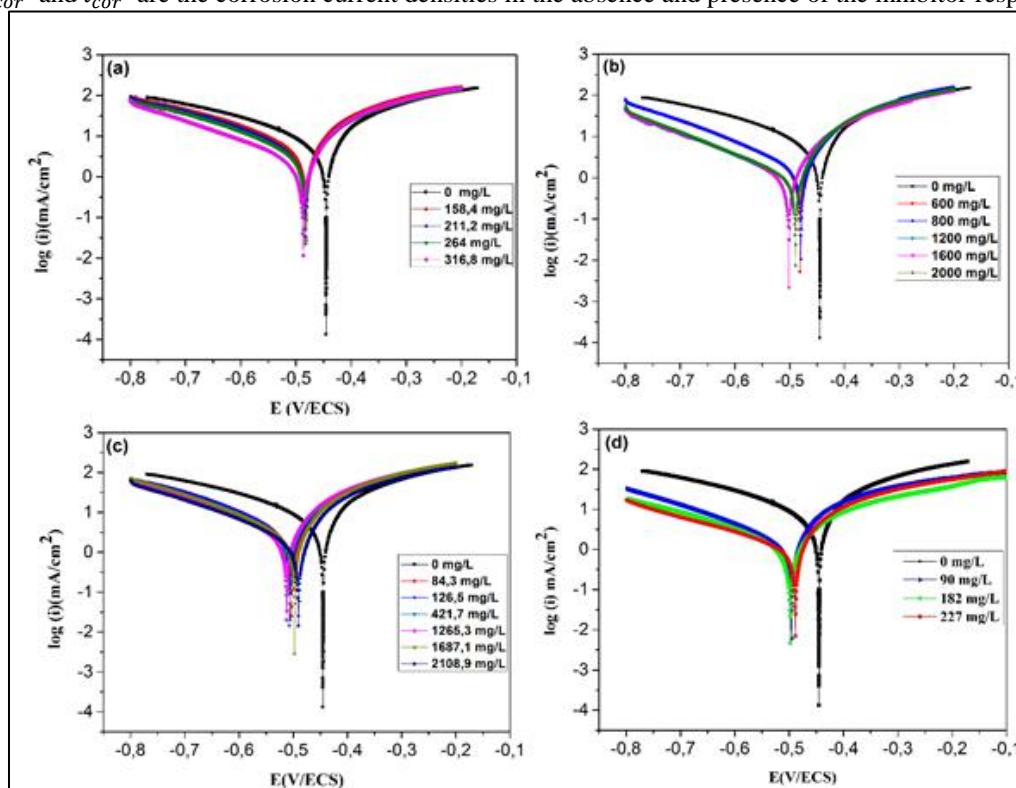


Figure 4: Tafel curve of X70 / H<sub>2</sub>SO<sub>4</sub> system at different concentration of solvent: MS2 (a); SS1 (b); SS2 (c); SS4 (d)

An inspection of the data in the Table 3 reveals, that at 25°C, addition of natural extract with different solvents, to the acid solution, the value of  $i_{cor}$  decreases significantly whereas the value of  $E_{cor}$  shifts slightly towards more negative direction. The largest displacement in  $E_{cor}$  value observed at concentrations of 1265.3 g/L with SS2 solvents is 64 mV, which is, much less than 85 mV. Thus, the magnitude of the displacement is not sufficient to ascertain the type of inhibitor being anodic or cathodic [20,21]. However, the polarization curves depicted in Figure 3 reveals that the cathodic curves are shifted towards lower current density side with increase in inhibitor concentration. This indicates that cathodic reaction is retarded on the addition of the extract and it should be defined as cathodic inhibitor. On the other hand, when  $\beta_a$  and  $\beta_c$  values are compared, it is observed that  $\beta_a$  values are significantly altered in presence of inhibitor, while  $\beta_c$  remains almost the same. Therefore, it may be inferred that the inhibitor retards the rate of anodic process probably through some other mechanism of adsorption. In the present situation, it is very difficult to decide whether it is the cathodic reaction which is predominantly retarded or the anodic reaction. Thus, it appears to be appropriate to define this inhibitor as mixed inhibitor.

The inhibition efficiencies obtained from the potentiodynamic polarization curves ( $E\%$ ) and EIS ( $\eta\%$ ) evolve in a similar way; however the efficiencies calculated from the EIS are lower. Indeed, despite the low rate of sites occupied by the adsorbed molecules (low  $\eta\%$ ), this assumes an intermolecular interactions type, between the adsorbed molecules, isolating the surface from the aggressive environment; therefore, a decrease in the overall corrosion current density (high  $E\%$ ).

Table 3: Electrochemical parameters of X70 in 0.5 M H<sub>2</sub>SO<sub>4</sub> in absence and presence of different extract solvents of the natural substance

	C (mg/L)	E <sub>corr</sub> (mV/SCE)	i <sub>corr</sub> (mA/cm <sup>2</sup> )	β <sub>a</sub> (mV/dec)	β <sub>c</sub>   (mV/dec)	E %
MS2	0	-448	6.9	136	243	-
	158.4	-481	5.21	89	221	24.47
	211.2	-481	5.16	88	220	25.27
	264	-482	3.23	80	192	53.18
	316.8	-487	2.05	68	192	70.32
SS1	600	-482	1.91	68	194	72.3
	800	-480	1.85	66	196	73.22
	1200	-502	1.26	71	207	81.77
	1600	-495	1.07	56	189	84.5
	2000	-490	1.07	54	194	84.5
SS2	84.3	-503	3.84	103	212	44.3
	126.5	-506	3.6	91	205	47.75
	421.7	-507	3.46	90	213	49.88
	1265.3	-512	2.74	78	203	60.19
	1687.1	-497	2.2	64	176	68.11
	2108.9	-490	1.6	60	175	76.72
SS4	90	-496	0.74	67	174	89.31
	182	-498	0.57	83	181	91.73
	227	-488	0.53	59	210	92.31

### Adsorption Isotherms

Sieverts and Lueg [22] established that the curves relating the corrosion rate of steel in acids and the concentration of organic inhibitors have the form of adsorption isotherms, suggesting an adsorption mechanism. Many adsorption isotherms for interpreting various research findings [23,24] exist; some of them are not amendable for use for adsorption of corrosion inhibitors. The models proposed by Langmuir, Temkin, Flory-Huggins, Frumkin, Freundlich and the so-called thermodynamic/kinetic (El-Awady et al.) isotherms are often applied to corrosion inhibitors.

In this work, various isotherms were tested and the Frumkin mode should be the best (Figure 5), where  $\Theta$  is the ratio  $\eta\%/100$  (Table 2). Frumkin adsorption isotherm is obtained according to the following equation:

$$\left(\frac{\theta}{1-\theta}\right) \exp(-2a\theta) = K C_{inh} \quad (6)$$

Where,  $\theta$  is the surface coverage of the metal surface,  $C_{inh}$  the inhibitor concentration and  $a$  used to predict the nature of interactions in the adsorbed layer. ( $a > 0$  lateral attraction and  $a < 0$  repulsion between adsorbed organic molecules),  $K$  is the equilibrium constant of the adsorption reaction given by:

$$K_{ads} = (1/1000)[\exp(-\Delta G_{ads}^0/RT)] \quad (7)$$

$\Delta G_{ads}^0$  is the adsorption energy,  $R$  is the gas constant,  $T$  is the absolute temperature, and, the value of 1000 in the above equation is the concentration of water in the solution in g/l, rather than 55.5 mole per liter because unit of concentration has been reported in terms of liter/g. It is very important to note that discussion of the adsorption isotherm behavior, using natural product extracts as inhibitors, in terms of the standard free energy of adsorption value, is not possible because the molecular mass of the extract components is not known. Some authors [25-27], in their study on acid corrosion with plant extracts, noted the same limitation. All correlation coefficient ( $R^2$ ) exceeded 0.99 indicates that the inhibition of X70 steel by extracts was attributed to adsorption of these compounds on the metal surface.



Thermodynamic parameters are listed in Table 4.  $K_{ads}$  denotes the strength between adsorbate and adsorbent. Large values of  $K_{ads}$  imply more efficient adsorption and hence better inhibition efficiency [28]. It is clear from the table that values of  $K_{ads}$  are low indicating weak interaction between the inhibitor and the X70 surface. It is seen that the values of 'a' are positive in all cases showing that attraction exists in the adsorption layer. This result explain the difference found between inhibition efficiencies obtained from the potentiodynamic polarization curves (E%) and EIS ( $\eta\%$ ).

The inhibition by the natural substance is due essentially to the laterals interactions between adsorbed molecules, rather than the number of anchoring sites of the adsorbed molecules. The negative values of  $\Delta G_{ads}^0$  ensure the spontaneity of the adsorption process and stability of the adsorbed layer on the steel surface. Generally, values of  $\Delta G_{ads}^0$  up to  $-20$  kJ.mol<sup>-1</sup> are consistent with electrostatic interactions between the charged molecules and the charged metal (physisorption) while those around  $-40$  kJ.mol<sup>-1</sup> or higher are associated with chemisorption. One can see that the calculated  $\Delta G_{ads}^0$  values, are less than  $-20$  kJ.mol<sup>-1</sup>, indicating therefore, that the adsorption mechanism of natural extracts on X70 in 0.5 M H<sub>2</sub>SO<sub>4</sub> solution was typical of physisorption.

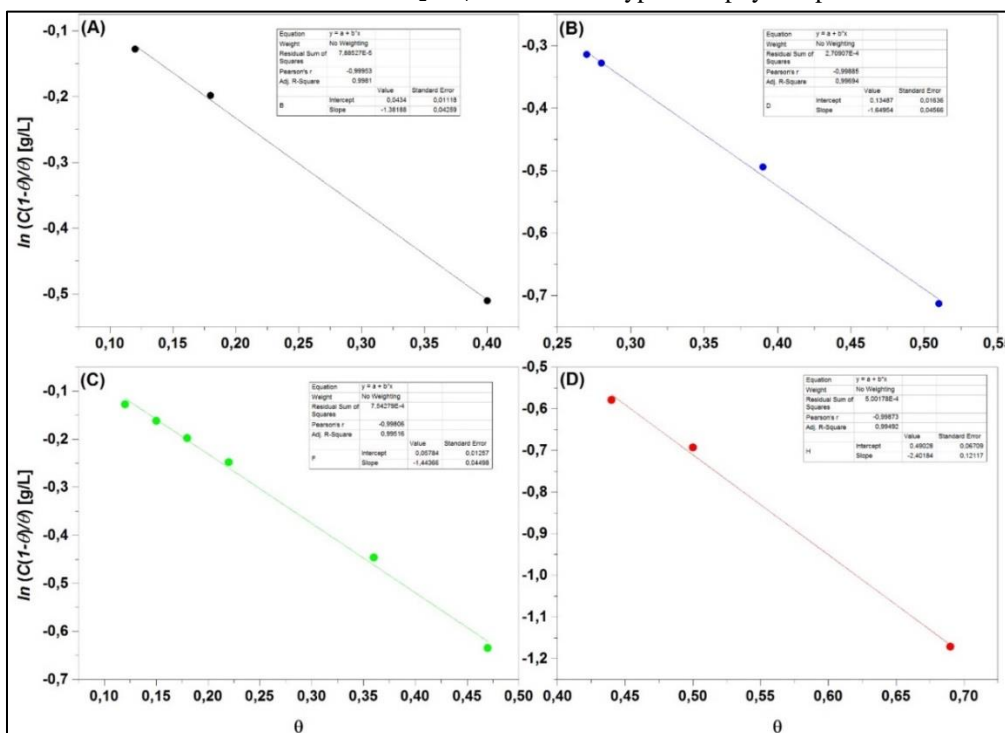


Figure 5: Frumkin adsorption plots obtained from EIS for X70 steel in 0.5 M H<sub>2</sub>SO<sub>4</sub> containing different concentrations of: MS2 (A); SS1 (B); SS2 (C); SS4 (D)

Table 4: Thermodynamic parameters for adsorption of inhibitors in H<sub>2</sub>SO<sub>4</sub> 0.5 M

Natural extract	<i>a</i>	$K_{ads}$	$\Delta G_{ads}^0$
MS2	0,69	0,96	-17,01
SS1	0,82	0,87	-16,78
SS2	0,72	0,94	-16,97
SS4	1,20	0,61	-15,90

### Effect of Temperature

The importance of temperature variation in corrosion study involving the use of inhibitors is to determine the mode of inhibitor adsorption on the metal surface. The aqueous extract of the pistachio galls by the solvent Methanol (SS4) has maximal efficiency around 92% at 227 mg/L, so the thermodynamic study was carried out with SS4 at its optimum concentration. The effect of temperature on the inhibition efficiency of X70 steel in 0.5 M H<sub>2</sub>SO<sub>4</sub> containing 227 mg/L of SS4 inhibitor, at temperature ranging from 25 to 55°C, and also in the absence of inhibitor,



was obtained with potentiodynamic polarization (Figures 6 and 7). Corresponding data are given in Table 5. As it can be seen, raising the temperature increases both the anodic and cathodic currents of X70 steel electrode, both in the absence and in the presence of SS4. It is seen from Table 5 that by increasing temperature, the corrosion current density ( $i_{\text{corr}}$ ) increases, although the investigated plant extract has demonstrated inhibiting properties at all studied temperatures. The addition of the extract in the  $\text{H}_2\text{SO}_4$  solution does not affect the  $E_{\text{corr}}$  values; however, there is no specific relation between  $E_{\text{corr}}$  and the increasing temperature. The inhibition efficiency of extract is enough satisfactory until  $45^\circ\text{C}$  and becomes less effective at  $55^\circ\text{C}$ .

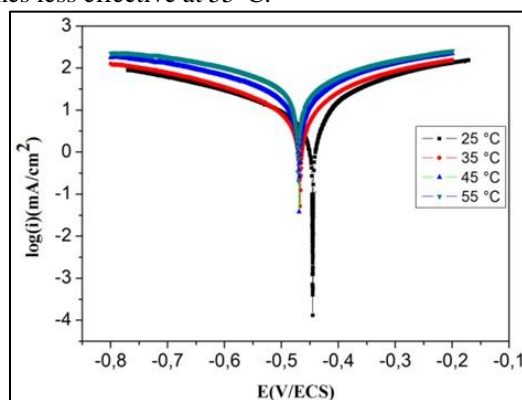


Figure 6: Polarization curves for X70 steel in 0.5 M  $\text{H}_2\text{SO}_4$  at different temperatures

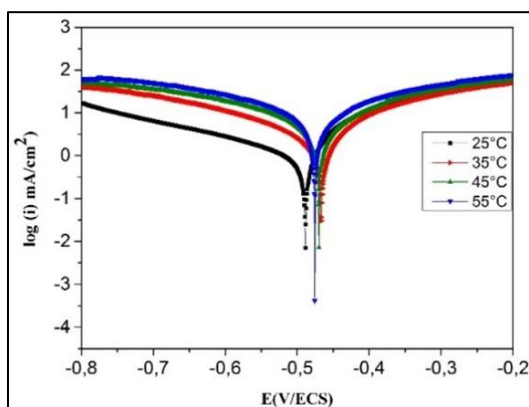


Figure 7: Polarization curves for X70 steel in 0.5 M  $\text{H}_2\text{SO}_4$  + 227 mg/L (SS4) at different temperatures

We were interested in the activation energy of the corrosion process and the kinetic parameters of the pistachio gall SS4 extract adsorption. In both the uninhibited and inhibited solutions, corrosion rate increased as temperature increased. The corrosion rate data were fitted into Arrhenius kinetic model (Eq. 8) and activation energy was elucidated from linear plots of  $\ln i_{\text{cor}}$  against reciprocal of temperature (Figures 8 and 9).

The obtained activation energy increased on addition of the inhibitor. Based on the concept of activation and collision theory, it can be considered that before the acid solution corrodes the steel, molecules of the acid must collide with the metal molecules on the surface. The acid molecules should possess energy up to a minimum threshold called the activation energy.

$$i_{\text{cor}} = A \exp\left(\frac{-E_a}{RT}\right) \quad (8)$$

In the presence of the extract, the activation energy values were higher than in the uninhibited solution (Table 6). Therefore, the acid molecules must acquire extra (higher) energy in the presence of inhibitor for corrosion to occur, hence corrosion inhibition. The increase in activation energy in the presence of inhibitor is consistent with trends reported in literature and is associated with physical adsorption mechanism [29].

Table 5: Polarization parameters and the corresponding inhibition efficiency for X70 steel in 0.5 M H<sub>2</sub>SO<sub>4</sub> in the absence and presence of 227 mg/L pistachio gall extract at different temperatures

Temperature (°C)	E <sub>corr</sub> (mV/SCE)	i <sub>corr</sub> (mA/cm <sup>2</sup> )	β <sub>a</sub> (mV/dec)	β <sub>c</sub>   (mV/dec)	E (%)
0.5 M H <sub>2</sub> SO <sub>4</sub>					
298.15	-448	6.9	136	243	-
308.15	-468	9.75	192	268	-
318.15	-470	20.01	201	273	-
328.15	-470	35.25	272	318	-
+ 227 mg pistachio gall					
298.15	-488	0.53	59	210	92.32
308.15	-466	3.11	149	240	88.62
318.15	-470	11.85	246	306	50.78
328.15	-477	30.54	282	323	13.36

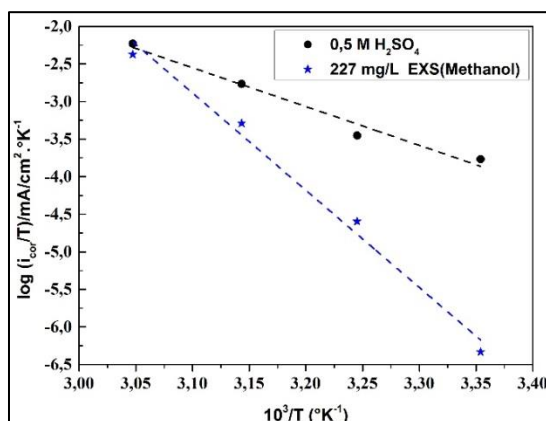


Figure 8: Arrhenius plots of  $\ln i_{cor}$  versus  $1/T$  for X70 in 0.5 M H<sub>2</sub>SO<sub>4</sub> in the absence and presence of SS4

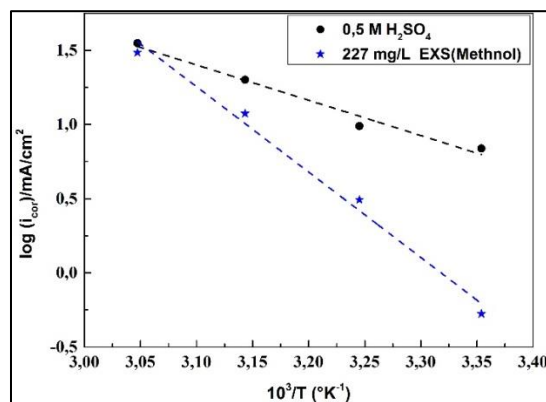


Figure 9: Arrhenius plots of corrosion corrosion  $\ln(i_{cor}/T)$  versus  $1/T$  for X70 in 0.5 M H<sub>2</sub>SO<sub>4</sub> in the absence and presence of extract  
An alternative formulation of Arrhenius equation is [30]:

$$i_{cor} = \frac{RT}{Nh} \exp\left(\frac{\Delta S_a}{R}\right) \exp\left(-\frac{\Delta H_a}{RT}\right) \quad (9)$$

Where,  $h = 6,6252 \cdot 10^{-34}$  J.s is Planck's constant,  $N$  is Avagadro's number,  $\Delta S_a$  is the entropy of activation and  $\Delta H_a$  is the enthalpy of activation. Figure 9 shows a plot of  $\ln \frac{i_{cor}}{T}$  vs.  $\frac{1000}{T}$ . Straight lines are obtained with a slope

of  $\frac{\Delta H_a}{R}$  and an intercept of  $\ln\left(\frac{R}{Nh}\right) + \frac{\Delta S_a}{R}$  from which the values of  $\Delta S_a$  and  $\Delta H_a$  are calculated and are given in Table 6.

The results showed positive sign for both  $E_a$  and  $\Delta H_a$ , reflecting the endothermic nature of corrosion process. It is obviously seen that the activation energy strongly increases in the presence of the inhibitor; some authors [31-33] attributed this result to the fact that the inhibitor species are physically adsorbed on the metal surface.  $\Delta S_a$  in the presence of the inhibitor is positive, meaning that an increase in disorder takes place in going from reactants to the activated complex [28]. On the other hand, with natural substances; it is not easy to confirm that all the molecules are adsorbed, some of them are more or less free, and therefore increases disorder.

Table 6: Activation parameters for X70 dissolution in 0.5 M H<sub>2</sub>SO<sub>4</sub> in the absence and presence of extract pistachio gall

	$E_a$ (kJ/mol)	$\Delta H_a$ (kJ/mol)	$\Delta S_a$ (J/mol.K)	Regression coefficient
0.5 M H <sub>2</sub> SO <sub>4</sub>	19.76	42.9	-85.75	0.9754
+ 227 mg pistachio gall	47,84	107.57	111.92	0.988

### FTIR Analysis of Corrosion Products in the Presence of Inhibitors

The products formed on the metal surface after the corrosion test in acid in the presence of different inhibitors, at their optimum concentrations, were analyzed using the FTIR spectrophotometer (Figure 10). Four X70 steel electrodes are immersed in a 0.5 M sulfuric acid solution supplemented with 316.8 mg/L of MS1, 2018.9 mg/L of SS2, 1600 mg/L of SS1 and 227 mg/L of SS4 respectively. 24 hours later, a layer of corrosion products is formed on the surface at each electrode, the layer is carefully pickled using a coverslip, and the four products obtained are then compressed into pellets in the presence of KBr and quickly analyzed by FTIR. Figure 10 shows the corrosion product and the corresponding pure extract. The IR spectra for the pure extraction solvents and the corrosion product show the same pattern. Which confirms that only the natural product extracts is involved in the inhibition process independently of the solvent. The role of the solvent is limited to the extraction of the active molecules; and to the obtaining of the plant extracts sufficiently rich in active molecules. The indexing spectra are as follows: the peak numbered 1 is assigned to the OH bond (3388-3455) cm<sup>-1</sup>, the peak numbered 2 is assigned to the molecule H<sub>2</sub>O (2354-2361) cm<sup>-1</sup>, the peak numbered 3 is assigned to the bond C = O (1635-1668) cm<sup>-1</sup>, the peak numbered 4 is assigned to the aromatic bond C = C (1463-1464) cm<sup>-1</sup>, the peak numbered 5 is assigned to the CO bond (1094-1105) cm<sup>-1</sup> and the peak numbered 6 is assigned to the aromatic CH bond (612-624) cm<sup>-1</sup>. All the groups present in the pure extracts are also present in corrosion product spectrum; this indicates the adsorption of the inhibitors MS1, SS2, SS3 and SS4 on the surface X70 steel. No new chemical bonds are formed between the metal and the natural substance; this confirms electrostatic type interactions.

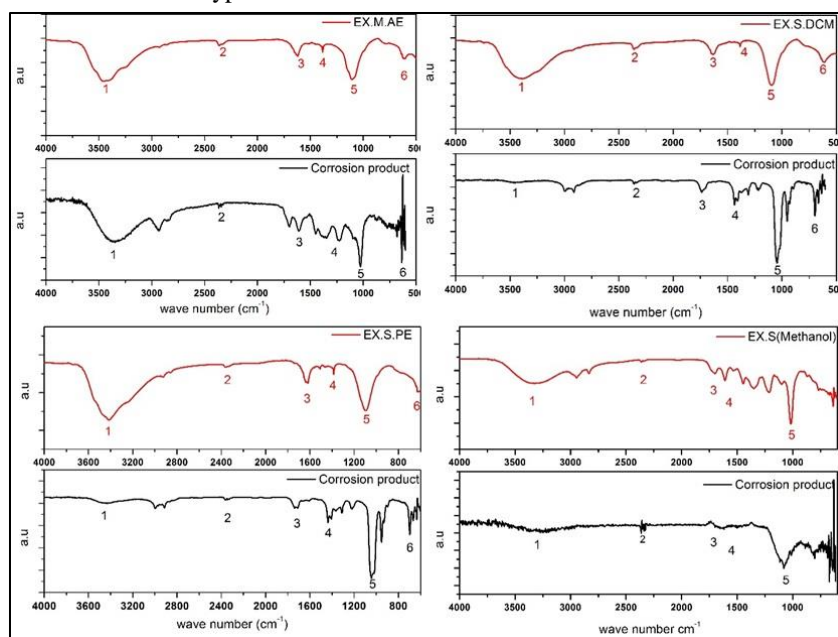


Figure 10: FTIR spectrum of surface product formed on the metal after the corrosion test in presence of inhibitor

## CONCLUSION

A new green inhibitor was extracted and studied as corrosion inhibitor for X71 steel in 0.5 M H<sub>2</sub>SO<sub>4</sub> solution. The essentials points of this work are as follows:

- 1) The use of natural substances as green corrosion inhibitors is conditioned by the solvent and method of extracting process. In the present work Soxhlet extraction using methanol offers the best yield of extract of pistachio galls (18.87%). The inhibition efficiency increases with increasing pistachio galls extract concentration and it depends on the solvent of extraction.
- 2) Tafel parameters reveal that the pistachio galls extract affects both anodic and cathodic reactions and acts more or less as a mixed inhibitor.
- 3) The best corrosion inhibition efficiency is about 92% it was recorded in the presence of 227 mg/L of SS4 extract in 0.5 M H<sub>2</sub>SO<sub>4</sub> solutions.
- 4) The extract under study resists corrosion effectively even at higher temperature. Inhibition efficiency is the best at 25°C and stays acceptable until 45°C, further increase in temperature results in decrease in inhibition efficiency.
- 5) The adsorption process follows the Frumkin adsorption isotherm with high correlation coefficient with all the studied extracts. The free energy and enthalpy of adsorption indicate that the adsorption of pistachio galls extract involves mainly the physical adsorption.
- 6) FTIR results provide direct evidence of adsorption of the extract on the surface of the steel. In addition, the inhibitory efficiency increases with interaction between the adsorbed molecules.

## REFERENCES

- [1] G Gökhan. *Corros Sci.* **2011**, 53(12), 3873-3898.
- [2] X Li; S Deng; H Fu; G Mu. *Corros Sci.* **2010**, 52(4), 1167-1178.
- [3] X Li; S Deng; H Fu; G Mu. *Corros Sci.* **2009**, 51(11), 2639-2651.
- [4] H Hachelef; A Benmoussat; A Khelifa; M Meziane. *J Fundam Appl Sci.* **2017**, 9(2), 650-668.
- [5] M Chellouli; D Chebabe; A Dermaj; H Erramli; N Bettach; N Hajjaji; MP Casaletto; C Cirrincione; A Privitera; A Srhiri. *Electrochimica Acta.* **2016**, 204, 50-59.
- [6] CG Dariva, AF Galio. Corrosion inhibitors—principles, mechanisms and applications. In: Developments in corrosion protection. InTech, **2014**.
- [7] Djemoui A; Souli L; Djemoui D; Okazi M; Naouri A; Rahmani S. *J Chem Pharm Res.* **2017**, 9(3), 311-318.
- [8] Ojha LK; Kaur K; Kaur R; Bhawsar J. *J Chem Pharm Res.* **2017**, 9 (6), 57-64.
- [9] Gupta NK; Verma C; Quraishi MA; Mukherjee AK. *J Mol Liq.* **2016**, 215, 47-57.
- [10] Ituen E; Akaranta O; James A; Sun S. *Sustainable Materials and Technologies.* **2017**, 11, 12-18.
- [11] Sifi I; Gourine N; Emile M; Yousfi Md. *Nat Prod Res.* **2015**, 29(20), 1945-1949.
- [12] Mecherara-Idjeri S ; Hassani A ; Castola V ; Casanova J. *J Essent Oil Res.* **2008**, 20(3) 215-219.
- [13] Ferhat M; Benchettara A; Amara SE; Najjar D. *J Mater Environ Sci.* **2014**, 5(4), 1059-1068.
- [14] Ahmed H; Tahar BM; Abdallah TM; Djamel B. *Eurasian J Anal Chem.* **2017**, 12(7) 977-986.
- [15] Ferhat M; Benchettara A; Amara SE. *J Fundam Appl Sci.* **2014**, 6(1), 92-105.
- [16] Karima T; Guibadj A; Taouti MB. *Eurasian J Anal Chem.* **2017**, 12(3), 275-294.
- [17] Khaled KF. *Electrochim Acta.* **2008**, 53(9), 3484-3492.
- [18] Chevalier M, Robert F, Amusant N, Traisnel M, Roos C, Lebrini M. *Electrochim Acta.* **2014**, 131, 96-105.
- [19] O Rahim; A Ben Chenna; T Zaiz; K Chaouch; T Lanez. *Rev Sci Fond App.* **2011**, 3(2), 85-98.
- [20] Mourya P; Banerjee S; Singh MM. *Corros Sci.* **2014**, 85, 352-363.
- [21] Soltani N; Tavakkoli N; Khayatkashani M; Jalali MR; Mosavizade A. *Corros Sci.* **2012**, 62, 22-135.
- [22] Sievert A; Lueg ZZ. *Anorg Chem.* **1923**, 126, 192.
- [23] Li W; He Q; Pei C; Hou B. *Electrochim Acta.* **2007**, 52(22), 6386-6394.
- [24] Zhang QB; Hua YX. *Electrochim Acta.* **2009**, 54(6), 1881-1887.
- [25] Faustin M; Maciuk A; Salvin P; Roos C; Lebrini M. *Corros Sci.* **2015**, 92, 287-300.
- [26] Li X; Deng S; Fu H. *Corros Sci.* **2012**, 62, 163-175.
- [27] Bobina M; Kellenberger A; Millet JP; Muntean C; Vaszilcsin N. *Corros Sci.* **2013**, 69, 389-395
- [28] Obot IB; Obi-Egbedi NO. *Colloids Surf A Physicochem Eng Asp.* **2008**, 330(2), 207-212.
- [29] Khadom AA ; Yaro AS; AlTaie AS; Kadum AA. *Portugaliae Electrochim Acta.* **2009**, 27(6), 699-712.

- [30] Quraishi MA; Singh A; Singh VK; Yadav DK; Singh AK. *Mat chem Phys.* **2010**, 122(1), 114-122.
- [31] Ashassi-Sorkhabi H; Shabani B; Aligholipour B; Seifzadeh D. *Appl Surf Sci.* **2006**, 252, 4039-4047.
- [32] Bouklah M; Benchat N; Aouniti A; Hammouti B; Benkaddour M; Lagrenée M; Vezin H; Bentiss F. *Prog Org Coat.* **2004**, 51, 118-124.
- [33] Ashassi-Sorkhabi H; Shaabani B; Seifzadeh D. *Appl Surf Sci.* **2005**, 239, 154-164.